Determinants of post-prandial plasma bile acid kinetics in human volunteers

Jarlei Fiamoncini[1]*, Andrianos M. Yiorkas[2,7]*, Kurt Gedrich[1], Milena Rundle[3], Sanne I. Alsters[2,7], Guus Roeselers[4,8], Tim J. van den Broek[4], Thomas Clavel[5], Ilias Lagkouvardos[6], Suzan Wopereis[4], Gary Frost[3], Ben van Ommen[4], Alexandra I. Blakemore[2,7], Hannelore Daniel[1].

1 - Department Food and Nutrition, Technische Universität München, Gregor-Mendel-Strasse 2, D-85354 Freising-Weihenstephan, Germany.
2 – Section of Investigative Medicine, Imperial College London, London, W12 0NN, UK.
3 – Division of Diabetes, Endocrinology and Metabolism, Department of Medicine, Imperial College London, Hammersmith Campus, London W12 0NN, UK
4 - TNO, Netherlands Institute for Applied Scientific Research, Microbiology & Systems Biology Group, Utrechtseweg 48, Zeist, The Netherlands
5 - Institute of Medical Microbiology, RWTH University Hospital, Pauwelsstrasse 30, Aachen, Germany
6 – Core Facility Microbiome/NGS, ZIEL Institute for Food and Health, Technische Universität München, Weihenstephaner Berg 3, D-85354 Freising-Weihenstephan, Germany
7 - Department of Life Sciences, Brunel University London, Middlesex, UB8 3PH, UK.
8 - Danone - Nutricia Research, Utrecht, The Netherlands.

*** - JF and AY share main authorship of this article**

Running head: Determinants of post-prandial plasma bile acid kinetics

Address for correspondence:
INRA - Centre de recherché Auvergne-Rhone-Alpes
Route de Theix
63122 Saint-Gènes Champanelle
France

Abstract

Bile acids (BA) are signaling molecules with a wide range of biological effects, also identified amongst the most responsive plasma metabolites in the post-prandial state. We here describe this response to different dietary challenges and report on key determinants linked to its inter-individual variability.

Healthy men and women (N=72, 62 ± 8 years) were enrolled into a 12-week weight loss intervention. All subjects underwent an oral glucose tolerance test (OGTT) and a mixed meal tolerance test (MMTT) before and after the intervention. BA were quantified in plasma by LC-MS/MS combined with whole genome exome sequencing and fecal microbiota profiling.

Considering the average response of all 72 subjects, no effect of the successful weight loss intervention was found on plasma BA profiles. Fasting and post-prandial BA profiles revealed high inter-individual variability and 3 main patterns in post-prandial BA response were identified using multivariate analysis. Although the women enrolled were postmenopausal, gender effects in BA response were evident. Exome data revealed the contribution of preselected genes to the observed inter-individual variability. In particular, a variant in the *SLCO1A2* gene, encoding the small intestinal BA transporter OATP1A2 was associated with delayed post-prandial BA increases. Fecal microbiota analysis did not reveal evidence for a significant influence of bacterial diversity and/or composition on plasma BA profiles.

The analysis of plasma BA profiles in response to two different dietary challenges revealed a high inter-individual variability, which was mainly determined by genetics and gender of host with minimal effects of the microbiota.

New and Noteworthy:

Considering the average response of all 72 subjects, no effect of the successful weight loss intervention was found on plasma BA profiles.

Despite high inter-individual variability, 3 main patterns in post-prandial BA response were identified using multivariate analysis.

A variant in the *SLCO1A2* gene, encoding the small intestinal BA transporter OATP1A2 was associated with delayed post-prandial BA increases to both the OGTT and MMTT.

Keywords: bile acids, *SLCO1A2*, post-prandial, OGTT, MMTT

Introduction

In addition to their role in solubilizing lipids in the intestine, bile acids (BA) are now recognized as important signaling molecules. They serve as ligands of the farnesoid X receptor (FXR) expressed in intestine and liver and thus control synthesis and transport of BA but also modulate expression of other genes(24, 28, 39, 43, 57, 64). After the discovery of a G protein-coupled receptor (TGR5) for BA(28, 39), acute metabolic effects of BA received considerable interest. With the expression of TGR5 and FXR in a wide range of cell types and tissues, BA effects cover immunomodulation, metabolism of adipose tissue and muscle as well as gastrointestinal hormone secretion (e.g. GLP-1)(27, 28). TGR5 activation by BA was shown to activate deiodinase, increasing the level of active thyroid hormone which in turn elevates the expression of enzymes involved in fatty acid oxidation in brown adipose tissue and skeletal muscle(24, 28, 39, 43, 57, 60, 64, 66). TGR5 was also identified as a target for treatment of obesity and type-2 diabetes. BA can (via farnesoid X receptor (FXR)-induced activation of short heterodimer partner (SHP) and its effect on hepatocyte nuclear factor 4 (HNF-4) and/or forkhead box O1 (Foxo1)) decrease the expression of gluconeogenic enzymes with a beneficial effect on glucose homeostasis in insulin resistance(28, 35, 38, 39). FXR also participates in the regulation of insulin synthesis and secretion as well as in the protection of pancreatic islets from lipotoxicity(27, 28, 44, 45). Via SREBP-1c activation, BA were also shown to modulate triacylglycerol synthesis in rodent liver(61).

Taken the relevance of BA as receptor ligands and their increase in circulation in the post-prandial state, it is remarkable that impressive differences in plasma levels of BA between individuals are not explained as yet. Within the NutriTech study, we recorded changes in BA plasma concentrations in 72 healthy male and female (postmenopausal) volunteers in response to an oral glucose tolerance (OGTT) and a mixed meal tolerance test (MMTT) combined with exome sequencing and fecal microbiota analysis. We here report on a large inter-individual variability of plasma BA profiles with pronounced gender effects and the identification of a number of gene variants underlying hepatic BA synthesis and enterohepatic recirculation.

Methods

1. Study design

The research project NutriTech was funded by the European Union 7 Framework program (clinicaltrials.gov record: NCT01684917). It aimed at better phenotyping human volunteers in response to standardized challenge tests. 72 volunteers (37 women and 35 men) in average 59.2±4.2 years-old, BMI 29.7±2.7, healthy at the screening considering fasting glucose and insulin concentrations and blood pressure values were recruited. The subjects underwent comprehensive phenotyping, including MRI scanning, food intake recording, and blood profiling for metabolites, hormones and chemokines. All subjects underwent an OGTT and a MMTT before and after a 12-week period, in which 40 participants followed a 20% caloric restriction diet while subjects in the control group consumed an average european diet which was matched for their energy expenditure to maintain body weight. Challenge tests always started at 09:00 am after 12 hours of fasting. The OGTT drink consisted of 75g glucose in 250 mL of water consumed within 5 minutes. Blood was collected in heparin-coated tubes at times 0, 15, 30, 60, 90, 120 and 240 minutes. The MMTT (also known as the “PhenFlex drink”) was a high-fat, high-glucose, high-caloric drink (400 ml) consisting of 320 ml tap water, 75g glucose, 60g palm olein, 20g profitar (protein supplement, Nutricia, Netherlands) and 0,5g artificial vanilla aroma resulting in a shake with 33, 59 and 8% of energy from carbohydrates, lipids and proteins, respectively. The drink was ingested within 5 minutes and blood was collected at 0, 30, 60, 120, 240, 360 and 480 minutes. Plasma was separated and stored at -80ºC for later analyses. Clinical chemistry parameters were assayed using enzymatic colorimetric kits and GLP-1 was measured using an in-house radioimmunoassay as previously described(30).

2. Bile acid analysis

Plasma bile acids were analyzed by a modified method originally described by Tagliacozzi et al (53). Briefly, 10 µL of plasma were mixed with 10 µL internal standard solution and 500 µL ice-cold methanol was added for deproteinization. Samples were vortexed and centrifuged at 15.000 g for 10 minutes. The supernatant was transferred to a 96 deep-well plate and evaporated under a stream of N_2. The solid remnants were re-suspended in methanol:water (1:1). Analysis was performed by LC-MS/MS using a triple quadrupole mass spectrometer (HPLC Agilent - CA, USA; QTrap 5500 - ABSciex MA, USA). BA were separated using a gradient with 0.2% formic acid in water and acetonitrile (acetonitrile going from 30 % at the start of the run to 100 % at 20 minutes) with a flow rate of 0.6 ml/min and

a reverse phase column (Phenomenex Luna C18(2) 150 x 4,6mm; 5µm particle size), kept at 40 °C. The mass spectrometer was operated in negative ion mode and mass spectra were obtained using the multiple reaction-monitoring mode (MRM). Integration of the peaks was done using Analyst Software (ABSciex MA, USA). Analyte concentration was calculated using deuterated internal standards (d4-Deoxycholic acid, d4-Glycoursodeoxycholic acid, d4-Glycodeoxycholic acid, d4-Glycocholic acid and d5-Taurocholic acid). Samples were randomized so that every batch contained samples from men and women, and from OGTT and MMTT performed before and after the intervention to avoid batch effects. Reference fasting plasma samples (Recipe Clinical Diagnostics Munich, Germany) were included in each batch and a dilution row of BA standards was processed in a similar manner in every batch for quantitation purposes. In total, 13 BA were quantified: ursodeoxycholic acid (UDCA), cholic acid (CA), chenodeoxycholic acid (CDCA), deoxycholic acid (DCA), glycoursodeoxycholic acid (GUDCA), glycocholic acid (GCA), glycochenodeoxycholic acid (GCDCA), glycodeoxycholic acid (GDCA), tauroursodeoxycholic acid (TUDCA), taurocholic acid (TCA), taurochenodeoxycholic acid (TCDCA), taurodeoxycholic aicd (TDCA) and taurolitocholic acid (TLCA). Due to the low abundancy and values below the lower limit of quantitation, UDCA TUDCA and TLCA were not taken into consideration in the statistical analysis. In our analyses, BA were grouped as primary (sum of CA, CDCA, and their taurine and glycine conjugates) or secondary + tertiary (DCA, LCA, UDCA including taurine and glycine conjugates thereof). The terms taurine-conjugated, glycine-conjugated, or unconjugated BA are used regardless of whether BA are primary or secondary + tertiary. In the text, total BA refers to the sum of all individual BA.

3. Exome DNA sequencing

Genomic DNA was extracted from saliva, collected using the Oragene® DNA sample collection kit (DNA Genotek, Ottawa, ON, Canada), following manufacturer's protocol. Whole-exome sequencing libraries were prepared from DNA using SureSelectXT Human All Exon V4+UTRs (71Mb) kit (Agilent Technologies, Santa Clara, CA). Sequencing was performed on a HiSeq25000 platform generating 100 base-pair end reads. After quality control using FastQC(29) version 0.10.0, sequencing reads were mapped to the GRCh37 (hg19) reference assembly of the human genome using BWA-MEM(36) version 0.7.2.(36) Variant calling was performed using GATK version 2.6(41) and quality filtered variants were annotated in ANNOVAR(58). Annotated exonic variants were filtered based on *in-silico*

predictive functional effects on the protein by two algorithms incorporated in the ANNOVAR suite: i) SIFT(31), which relies on the degree of conservation of amino acid residues in highly conserved regions in sequence alignments derived from closely related sequences and ii) Polyphen-2(2) which predicts the possible impact of amino acid substitutions on the stability and function of human proteins using structural and comparative evolutionary considerations. These approaches indicate a high probability that an amino acid change is "deleterious" based on a combination of these attributes. The effect of the identified variants on post-prandial BA metabolism was analyzed by creating allelic gene scores, which represented the sum of deleterious variants per gene involved in BA synthesis, metabolism and transport. Where necessary individual variants were analyzed separately.

4. High-throughput microbiome 16S rRNA gene amplicon sequencing

Fresh stool sample were collected by subjects before and after a 12-week intervention period. Samples were immediately frozen at −20 °C by the subjects after defecation and transported in frozen state to the laboratory at TNO where samples were mechanically homogenized, split into aliquots in sterile 2 ml cryovials and stored at −80 °C. For fecal genomic DNA isolation, approximately 100-150 mg of fecal material was directly transferred to DNA isolation plates. Phenol pH8.0 was added and the samples were mechanically disrupted by bead beating with a 96-well plate Beadbeater (Biospec Products, Bartlesville). Isolated DNA was extracted and purified with the AGOWA mag Mini DNA Isolation Kit (AGOWA, LGC genomics, Berlin, Germany) as described in Kelder et al (2014)(29). Microbiota analysis was performed by high-throughput sequencing of bar-coded amplicons spanning the archaeal and bacterial V4 hypervariable region. These amplicons, generated from a standardized quantity of template DNA (100pg) using adapted primers 515F and 806R, were bidirectionally sequenced using the MiSeq system (Illumina, San Diego, CA) as described previously(11).

Data were analysed as described in detail previously(33). Raw reads were processed using an in-house developed pipeline (www.imngs.org)(32) based on the UPARSE approach(16). Sequences were trimmed to the first base with a quality score <3 and then paired. Those with less than 200 and more than 300 nucleotides and paired reads with an expected error >3 were excluded from the analysis. Remaining reads were trimmed by five nucleotides on each end to avoid GC bias and non-random base composition. The presence of chimeras was tested using UCHIME(15). Operational taxonomic units (OTUs) were clustered at 97% sequence similarity, and only those with a relative abundance >0.5% in at least one sample

were kept. Taxonomies were assigned at 80% confidence level using the RDP classifier(59).

5. Statistical analysis

Depending on the nature of comparisons, T-test, 1-way ANOVA or 2-way ANOVA with post hoc multiple comparison Bonferroni's test were used. Unless otherwise stated, differences with $P<0.05$ were considered as significant. Shapiro-Wilk test was used to assess normality. Results from calculation of area under the curve (AUC), refers to incremental AUC, which considers individual values at t=0 as baseline. In cases where outliers where removed, their detection was done using ROUT method.

The contribution of individual predictors to the overall variation of plasma BA concentrations was quantified by means of percentaged marginal coefficients of determination (R^2) which were obtained by means of ANOVA using a Mixed Design Model taking into account repeated measures per subject during the MMTT. Individual predictors included allelic gene scores, microbiota families, gender and MMTT time points. For this analysis, family level microbiota data were used with a relative abundance of >0.5% in at least 30 % of the samples. Analysis at lower taxonomic ranks is not compatible with the classification confidence of short reads and the taxonomic incongruence of some dominant and prevalent bacterial genera in the human gut.

Statistical analysis of microbiota profiles was performed in the R programming environment using Rhea (https://lagkouvardos.github.io/Rhea/)(32). OTU tables were normalized to account for differences in sequence depth. ß-diversity was computed based on generalized UniFrac distances(12) while α-diversity was assessed on the basis of species richness and Shannon effective diversity(26). For de novo clustering of microbiota profiles, Partitioning Around Medoids was performed as described previously(7).

Results

Effect of the intervention on plasma bile acids

All subjects underwent the OGTT and MMTT challenges two times, separated by 12 weeks of weight loss intervention. While a subgroup of volunteers (n=32) followed a supervised diet to keep body weight constant, 40 volunteers followed a diet with a 20% energy restriction that led to a mean weight loss of 5.6 kg. This weight loss however did not cause any significant changes in fasting glucose or insulin concentrations (data not shown) nor did it change the composition and concentrations of circulating BA in fasting state and during the dietary challenges (Figure 1). Based on the lack of an effect of the weight-loss we calculated and used the mean values of the BA concentrations during the OGTT and MMTT. In this way we minimized variation and could overcome problems caused by eventual missing samples.

Fasting plasma BA levels

Quantification of the most abundant BA species in plasma (collected between 08:00 and 09:00am after 12h of fasting) revealed a high inter-individual variability in both concentrations as well as composition. For the sum of all BA, a 12-fold difference across the 72 volunteers was found. Glycine-conjugated BA accounted for around 47% and taurine-conjugated species for around 7% of the total BA pool, while unconjugated species represented 46% of total (Figure 2 and Figure 3G and 3H time point 0). Primary BA were more abundant than the sum of secondary + tertiary and corresponded to approximately 60% of the total BA pool.

Post-prandial responses of plasma BA to OGTT and MMTT

The mean total plasma BA concentration increased 3.3-fold in response to the MMTT (Figure 3A) with maximal levels reached after 1 hour and remaining constant for up to 6 hours. Even at 8 hours after consumption of MMTT test drink, concentrations were on average 1.7-fold higher than in overnight fasting state. Bile acid concentrations also increased during the OGTT but here peak concentrations were reached after 30 minutes with levels on average 2-fold higher than in fasting state (Figure 3A). After 90 minutes BA concentrations started to decline to reach fasting state levels after 240 minutes.

Different classes of BA displayed different kinetic behaviors. Based on mean values of all volunteers, primary BA increased by 3.9-fold during the MMTT and by 2.1-fold during the OGTT. Secondary + tertiary BA showed a lower response with a maximal increase of 2.8-

fold during the MMTT and 1.8-fold during the OGTT compared to fasting levels (Figures 3B and 3C). In the OGTT and MMTT, levels of glycine- and taurine-conjugated BA increased around 5-fold in the MMTT and around 3-fold in the OGTT (Figures 3D and 3E). Plasma concentration of unconjugated BA showed only a small increase during MMTT (1.6-fold at 240 min) and even a 15% decrease at the end of the OGTT (Figure 3F). A shift in the composition of circulating BA was observed in the transition from fasting to postprandial state. Glycine-conjugated BA – comprising 47% of the total BA pool in fasting state - increased to 68% during the MMTT and the taurine-conjugated species went from 7% to 11%, while unconjugated entities declined from 46% to 20% after 2h in the MMTT (Figure 3H). A very similar change in composition was observed during the OGTT, although in this case, the increase in glycine-conjugated BA (and concomitant decline in unconjugated species) was less pronounced (Figure 3G).

Gender-specific differences in post-prandial BA responses

During OGTT, plasma BA concentrations increased similarly in men and women, reaching maximum values after 30 and 60 minutes, respectively. Women thereafter sustained maximal concentrations of BA for at least 2 hours, whereas in men concentrations were significantly reduced already at 90 minutes (P=0.0011) as shown in Figure 4A. The gender-specific differences in response to the OGTT were particularly evident when inspecting the glycine- and taurine-conjugated BA (P<0.0001 and P=0.0098 for differences in AUC for taurine- and glycine-conjugated BA, respectively), as demonstrated in Figures 4B and 4C. Although less pronounced than in the OGTT, gender-related differences were also observed in response to the MMTT, but only for taurine-conjugated BA (P=0.0085 for difference in AUC) as shown in Figure 4F. Despite these post-prandial gender differences, overnight fasting BA concentrations were similar between men and women.

Clusters of post-prandial BA responses

Not only fasting BA concentrations but also post-prandial changes in plasma BA displayed large inter-individual variability. There was no correlation between the AUC of post-prandial total BA with their fasting concentration (data not shown).

As compared to an average 3.3-fold increase in circulating total BA levels following the MMTT, some subjects responded with a more than 10-fold increase, whereas others barely showed any change. A hierarchical clustering approach based on BA concentration profiles in response to the MMTT identified 3 subgroups of volunteers with an almost equal

distribution of men and woman in each cluster. These significant differences in plasma BA kinetics are shown in Figures 5A and 5B. Different classes of BA displayed distinct kinetic behaviors, particularly when unconjugated BA were compared to conjugated species. In cluster 1 (n=35), post-prandial BA concentrations increased on average 4.3-fold with a maximum reached within the first hour. Even after 8 hours, in this cluster BA concentrations were 2.3-fold higher than in fasting state. In cluster 3 (n=21), fasting levels of BA were almost twice as high as in other clusters but here subjects displayed a slower increase in plasma profiles with maximal values of around 2.9-fold of fasting state after 4 hours, returning to fasting state concentrations after 8 hours. Subjects in cluster 2 (n=13) displayed a completely different kinetic profile with plasma concentrations increasing to a maximum of 4.6-fold of fasting levels at 6 hours, and even after 8 hours levels were still 3.4-fold higher than in fasting state.

Determinants of BA profiles

To identify some of the determinants underlying the different BA kinetics, host genome and fecal microbiota sequencing approaches were used. Exome sequencing data were analyzed for genetic heterogeneity in target genes identified by knowledge and GO-classification for a subset of 60 genes involved in hepatic BA synthesis, enterohepatic recirculation, and transmembrane transport of BA. A list of these genes screened for variations is provided on Table 1. Subjects were grouped according to the presence of variants known or predicted to impair protein functionality defined as “deleterious” based on SIFT and Polyphen-2 algorithms. Although various gene variants revealed associations with plasma BA profiles (Table 2), those in the *SLCO1A2* gene were observed in a number of volunteers large enough to allow a reliable association with phenotype. *SLCO1A2* encodes the organic anion-transporting polypeptide-1 A2 (OATP1A2), which mediates BA uptake across the apical membrane of enterocytes in upper small intestine but also in distal nephrons, cholangiocytes and at the blood brain barrier(10, 21). In this gene, a previously described functional polymorphism rs11568563 (c.A516C, p.E172D, MAF=0.03) was found in 9 out of 72 subjects and an additional rare variant rs368672331 (c.G727A, p.G243S) was found in another subject. All rs11568563 carriers displayed a delayed post-prandial increase of conjugated BA in plasma compared to the other volunteers not bearing this variant (Figure 6). Variants in the *SLC10A2* gene that encodes the apical sodium-dependent bile acid transporter (ASBT) in ileum (considered the prime site for BA reabsorption) such as rs71640248, rs117447044 and rs56398830 were also found in 4

volunteers that as well showed reduced postprandial increases in BA concentrations (data not shown).

Multivariate analyses providing marginal R^2 showed that a substantial proportion of the variation in BA concentration profiles could be attributed to the time point of measurement during the MMTT, gender, selected SNPs and microbiota (Table 2). Across all individual parameters, the lowest cumulative values were found for the cholic acid conjugated species TCA and GCA with 37 and 43% of total variation explained, whereas the highest values were calculated for DCA and its glycine and taurine-conjugates with 69, 63 and 64% of variance explained. Up to 50% of total variation could be attributed to the selected SNPs, particularly in case of DCA and its taurine and glycine conjugates. Variants in the gene encoding Epoxide hydrolase 1 (EPHX1) were found in 39 subjects and this gene alone accounted for 14% of variation in DCA concentrations and approximately 30% of variation in concentrations of its conjugates GDCA and TDCA. Additional individual effects (particularly for unconjugated primary BA) were found for the canalicular multispecific organic anion transporter ABCC3, the racemase AMACR that can interconvert BA as well as for the BA receptor TGR5 encoded by GPBAR1 (variants found in 6 subjects) and for a putative phospholipid-transporting ATPase encoded by ATP8B1, which displayed deleterious variants in 26 volunteers. Given the small size of the study population and the small number of carriers of individual variants no other attempts were made to associate phenotype and genotypes.

Gender was particularly associated with the concentrations of taurine-conjugated BA. Most of the selected gut bacterial families had only a marginal effect on BA concentrations, with the exception of *Coriobacteriaceae*, *Erysipelotrichaceae*, and most notably *Peptostreptococcaceae,* which accounted for 12% of variation in CA concentrations. Whereas the family *Coriobacteriaceae* is known to include bile acid-converting species(46, 62), results pertaining to the *Peptostreptococcaceae* require additional studies.

To further assess the possible influence of gut microbiota in a non-supervised manner, *de novo* clustering of fecal microbial profiles based on phylogenetic distances revealed the presence of three distinct clusters of individuals (Figure 7). Each of these clusters was characterized by significant differences in alpha-diversity and in the relative abundance of specific taxa (data not shown), but supervised multidimensional analysis of BA kinetics parameters on the basis of these microbiota-derived clusters followed by statistical tests on individual BA parameters did not reveal any significant associations. Likewise, comparison

of the fecal microbiota of individuals belonging to the three different BA-specific clusters (Figure 5) did not show significant differences in any of the bacterial taxonomic groups identified (data not shown).

Discussion

The high inter-individual variability of plasma BA levels and composition in the fasting and post-prandial states found in our study confirms previous observations(9, 18, 52). This high variability has intrinsic and extrinsic origins. BA synthesis rate, intestinal absorption and hepatic processing, as well as bacterial metabolism are just a few factors that may contribute to the variability. In addition, acute and chronic effects of diet or drug use and also diurnal variation(14, 18) are known to affect the BA pool. Given the fact that dozens of proteins are involved in BA synthesis and handling in the mammalian system, it can be anticipated that there are also numerous underlying genetic factors. Nies et al. attributed the high inter-individual variability specifically to differences in the expression of transporters involved in hepatic BA transport such as OATP1B1, OATP1B3 and OATP2B1(42). Although no systematic study has explored SNPs or haplotypes in relation to post-prandial plasma BA profiles, a recent study identified epistatic effects in primary BA biosynthesis by employing an Empirical Bayesian Lasso approach for analysis of pathway-based GWAS data(25).

Based on blood sampling up to 4 (OGTT) or even 8 hours postprandially in the case of MMTT, distinct kinetic profiles of individual BA species were observed. Maximal increases in plasma levels exceeding fasting concentrations up to 4.6-fold for taurine- as well as glycine-conjugated BA were found at 30 min in the OGTT with sustained levels for over 2 hours. These changes match well to those reported previously by others(49),(65). In a study with 73 young volunteers (26 ± 4 years-old), Matysik et al. demonstrated a rise in glycine- and taurine-conjugated BA with a peak at 60 minutes after glucose ingestion, although there was no blood sampling at earlier time points(40). Interestingly, Zhao et. al. reported a biphasic increase in plasma BA, with the first peak at 30 minutes and a second peak at 120 minutes(65). Although the mean plasma levels in our study did not reveal a biphasic behavior, some volunteers clearly presented 2 distinct peaks in BA profiles. The fast appearance of the BA in blood during the OGTT - which in essence can be superimposed onto the rise in blood glucose levels (Figure 6C and 6F) - suggests a very rapid uptake of BA in the upper small intestine. Absorption in the duodenum and jejunum is generally not considered as relevant and is postulated to occur by passive diffusion of protonated BA species(13, 54). The main site of BA reuptake and delivery into portal circulation is thought to be the ileum with apical influx via the Na^+-dependent *SLC10A2* (ASBST) transporter. Our results however strongly argue for absorption of a considerable quantity of BA already in

duodenum and jejunum. This applies also for the conjugated BA, since maximal plasma concentrations were observed here at 30 minutes in response to during the OGTT and at 60 minutes in response to the MMTT, when the majority of ingested nutrients not even have reached the ileum (Figure 3).

The presence of glucose in the intestinal lumen is known to elicit a cholecystokinin (CCK) secretion(37) followed by gallbladder contraction. A rise in plasma BA levels in response to the OGTT is thus per se not surprising. Since BA are not required for glucose absorption, BA secretion may therefore be taken as an archaic evolutionary response with glucose sensing as a surrogate for ingested food. CCK secretion is far stronger in response to a mixed meal and was shown to increase proportional to the lipid content of the meal(37, 50). Increasing CCK-output translates into differences in gallbladder emptying and corresponding plasma BA changes(50, 51). Although we did not determine CCK-levels and gallbladder ejection fraction, it is very reasonable to assume the responses to the OGTT and MMTT in our volunteers was very similar to those described in other studies[44]. Conjugated BA are the most abundant in bile(3, 47) and consequently the post-prandial plasma changes of these BA as compared to the other species were much more pronounced. Concentrations of unconjugated BA only mildly increased in a small subset of subjects after 6 hours in response to the MMTT.

It was previously reported that the increase in plasma levels of conjugated BA in response to OGTT and oral lipid tolerance tests are higher in women than in men(23, 48), while no differences are reported in most studies for the fasting state(9, 19, 63). Also in mice, gender effects in the BA pool were observed and those were related to different expression levels of BA biosynthetic enzymes(17, 55). Although all women enrolled in our study were post-menopausal, significant differences in post-prandial levels of conjugated BA were still detectable between men and women, particularly for taurine-conjugated BA during the OGTT, but also during the MMTT.

Bile acids quantified in systemic circulation are basically the spillover of a non-complete hepatic extraction of BA in first pass(6, 24). Their concentration in peripheral blood is thus the result of a series of connected processes with secretion from the gallbladder into intestine, transit and absorption across apical and basolateral membranes of enterocytes into portal blood followed by hepatic uptake and biliary secretion. Variability in individual components within this sequence of events will eventually define the shape of the temporal plasma BA profile following a meal. We could group our volunteers based on the post-

prandial kinetic profiles into 3 main clusters with different velocities in plasma appearance and absolute concentrations of BA.

It can be expected that these differences in plasma BA profiles in response to dietary challenges lead to alterations in physiological processes sensitive to BA. It is known that GLP-1(22, 27, 56) and insulin(1) secretion as well as substrate oxidation (demonstrated in rodents) are subject of regulation by BA. And, indeed, we observed an association of post-prandial total plasma BA and GLP-1 concentrations during the OGTT (Figure 8). When volunteers were clustered according to the increase in plasma levels of glycine-conjugated BA during the first hour of the OGTT, significant differences between the high and low responders were observed for circulating GLP-1 levels. This suggests that the rise in GLP-1 initiated by glucose administration may be modulated by BA released into the intestine of by circulating BA reaching enteroendrocine cells (Figure 8C). The effect was most prominent for glycine-conjugated BA as the responsive BA category which also has the highest circulating concentrations. This relationship between BA secretion and corresponding GLP-1 levels was however not observed in the MMTT (Figure 8 D). The MMTT drink also contained lipids and proteins that can also promote GLP-1 secretion, resulting in a 2-fold higher plasma GLP-1 and BA levels as compared to the OGTT. Lipids and proteins seem to promote a stronger GLP-1 output that may overrule the BA modulatory effects on GLP-1 secretion during the MMTT.

One of the most important outcomes of the present study is that genetic variants in the BA transporter OATP1A2 associate with differences in postprandial BA kinetics but not the overnight fasting plasma BA levels. Carriers of the nonsynonymous SNP (c.A516C, p.E172D) in the *SLCO1A2* gene displayed significantly lower plasma BA concentrations in response to the OGTT and during the first hours of the MMTT, indicating reduced and delayed absorption of BA from intestine. Since OATP1A2 is expressed in the duodenum(4, 20) it is the candidate transporter that could mediate the early phase of BA absorption leading to rapid changes in plasma BA levels as observed in response to the OGTT in which peak BA levels can be superimposed on glucose peaks. The A516C variant of *SLCO1A2* was demonstrated to markedly reduce the transport capacity for different substrates when expressed heterologously(8, 34) although this has not been shown for BA as substrates. Post-prandial concentrations of unconjugated BA, which are thought to be taken up into enterocytes via diffusion (not depending on transporters) were not affected in volunteers with the A516C variant, corroborating the importance of this transporter for

454 duodenal BA transport. Although BA concentrations could not be measured in portal blood
455 in the present study, BA in systemic circulation are considered as a surrogate of
456 enterohepatic circulation (5), corroborating our hypothesis of a slower intestinal BA uptake
457 in carriers of the deleterious variation in *SLCO1A2*.

458 Taken together, our study describes different BA kinetics following an OGTT and a MMTT
459 and identified key determinants underlying the large inter-individual variability in
460 postprandial BA profiles. The different patterns of post-prandial BA responses, associated
461 with fasting concentrations of BA allowed the classification of the 72 subjects into the 3
462 major clusters or “metabotypes”. The finding that heterogeneity in 60 preselected genes of
463 BA synthesis and transport explained most of the BA variance argues for these
464 metabotypes as mainly genetically determined and not too much dependent on gut
465 microbiota structure as measured by amplicon sequencing in spite of the known
466 involvement of specific bacterial species in bile acid metabolism in the intestine. Finally, the
467 present study is the first to demonstrate an association between a common genetic variant
468 in the OATP1A2 transporter and post-prandial BA kinetics, despite the absence of any
469 effects in the fasting state. Understanding the metabolism of BA in the post-prandial state is
470 essential to better understand their roles in human physiology.

471

472 **Acknowledgement:** The excellent technical work of Alexander Haag, Ronny Scheundel
473 and Barbara Gelhaus is highly appreciated.

474 JF current affiliation: INRA, UMR 1019, UNH, CRNH Auvergne, F-63000 Clermont-Ferrand;
475 Clermont Université, Université d'Auvergne, Unité de Nutrition Humaine, BP 10448, F-
476 63000 Clermont-Ferrand, France

477

478 **Grants:** The authors are thankful for the funding received through the EU 7th Framework, to
479 all study participants and all members of the NutriTech consortium. The microbiota analysis
480 was funded by the TNO Systems Biology program.

481

References

1. **Adrian TE**, **Gariballa S**, **Parekh KA**, **Thomas SA**, **Saadi H**, **Kaabi Al J**, **Nagelkerke N**, **Gedulin B**, **Young AA**. Rectal taurocholate increases L cell and insulin secretion, and decreases blood glucose and food intake in obese type 2 diabetic volunteers. *Diabetologia* 55: 2343–2347, 2012.

2. **Adzhubei I**, **Jordan DM**, **Sunyaev SR**. Predicting functional effect of human missense mutations using PolyPhen-2. *Curr Protoc Hum Genet* Chapter 7: Unit7.20, 2013.

3. **Alnouti Y**, **Csanaky IL**, **Klaassen CD**. Quantitative-profiling of bile acids and their conjugates in mouse liver, bile, plasma, and urine using LC-MS/MS. *J Chromatogr B Analyt Technol Biomed Life Sci* 873: 209–217, 2008.

4. **Amelsberg A**, **Jochims C**, **Richter CP**, **Nitsche R**, **Fölsch UR**. Evidence for an anion exchange mechanism for uptake of conjugated bile acid from the rat jejunum. *Am J Physiol* 276: G737–42, 1999.

5. **Angelin B**, **Björkhem I**, **Einarsson K**, **Ewerth S**. Hepatic uptake of bile acids in man. Fasting and postprandial concentrations of individual bile acids in portal venous and systemic blood serum. *J Clin Invest* 70: 724–731, 1982.

6. **Angelin B**, **Einarsson K**, **HELLSTROM K**. Evidence for the absorption of bile acids in the proximal small intestine of normo- and hyperlipidaemic subjects. *Gut* 17: 420–425, 1976.

7. **Arumugam M**, **Raes J**, **Pelletier E**, **Le Paslier D**, **Yamada T**, **Mende DR**, **Fernandes GR**, **Tap J**, **Bruls T**, **Batto J-M**, **Bertalan M**, **Borruel N**, **Casellas F**, **Fernandez L**, **Gautier L**, **Hansen T**, **Hattori M**, **Hayashi T**, **Kleerebezem M**, **Kurokawa K**, **Leclerc M**, **Levenez F**, **Manichanh C**, **Nielsen HB**, **Nielsen T**, **Pons N**, **Poulain J**, **Qin J**, **Sicheritz-Ponten T**, **Tims S**, **Torrents D**, **Ugarte E**, **Zoetendal EG**, **Wang J**, **Guarner F**, **Pedersen O**, **de Vos WM**, **Brunak S**, **Doré J**, **MetaHIT Consortium**, **Antolín M**, **Artiguenave F**, **Blottiere HM**, **Almeida M**, **Brechot C**, **Cara C**, **Chervaux C**, **Cultrone A**, **Delorme C**, **Denariaz G**, **Dervyn R**, **Foerstner KU**, **Friss C**, **van de Guchte M**, **Guedon E**, **Haimet F**, **Huber W**, **van Hylckama-Vlieg J**, **Jamet A**, **Juste C**, **Kaci G**, **Knol J**, **Lakhdari O**, **Layec S**, **Le Roux K**, **Maguin E**, **Mérieux A**, **Melo Minardi R**, **M'rini C**, **Muller J**, **Oozeer R**, **Parkhill J**, **Renault P**, **Rescigno M**, **Sanchez N**, **Sunagawa S**, **Torrejon A**, **Turner K**, **Vandemeulebrouck G**, **Varela E**, **Winogradsky Y**, **Zeller G**, **Weissenbach J**, **Ehrlich SD**, **Bork P**. Enterotypes of the human gut microbiome. *Nature* 473: 174–180, 2011.

8. **Badagnani I**, **Castro RA**, **Taylor TR**, **Brett CM**, **Huang CC**, **Stryke D**, **Kawamoto M**, **Johns SJ**, **Ferrin TE**, **Carlson EJ**, **Burchard EG**, **Giacomini KM**. Interaction of methotrexate with organic-anion transporting polypeptide 1A2 and its genetic variants. *J Pharmacol Exp Ther* 318: 521–529, 2006.

9. **Bathena SPR**, **Thakare R**, **Gautam N**, **Mukherjee S**, **Olivera M**, **Meza J**, **Alnouti Y**. Urinary bile acids as biomarkers for liver diseases I. Stability of the baseline profile in healthy subjects. *Toxicol Sci* 143: 296–307, 2015.

10. **Bronger H**, **König J**, **Kopplow K**, **Steiner H-H**, **Ahmadi R**, **Herold-Mende C**, **Keppler D**, **Nies AT**. ABCC drug efflux pumps and organic anion uptake transporters in human gliomas and the blood-tumor barrier. *Cancer Res* 65: 11419–11428, 2005.

11. **Caporaso JG**, **Lauber CL**, **Walters WA**, **Berg-Lyons D**, **Huntley J**, **Fierer N**, **Owens SM**, **Betley J**, **Fraser L**, **Bauer M**, **Gormley N**, **Gilbert JA**, **Smith G**, **Knight R**. Ultra-high-throughput microbial community analysis on the Illumina HiSeq and MiSeq platforms. *ISME J* 6: 1621–1624, 2012.

12. **Chen J**, **Bittinger K**, **Charlson ES**, **Hoffmann C**, **Lewis J**, **Wu GD**, **Collman RG**, **Bushman FD**, **Li H**. Associating microbiome composition with environmental covariates using generalized UniFrac distances. *Bioinformatics* 28: 2106–2113, 2012.

13. **Dawson PA**, **Lan T**, **Rao A**. Bile acid transporters. *J Lipid Res* 50: 2340–2357, 2009.

14. **Duane WC**, **Levitt DG**, **Mueller SM**, **Behrens JC**. Regulation of bile acid synthesis in man. Presence of a diurnal rhythm. *J Clin Invest* 72: 1930–1936, 1983.

15. **Edgar RC**, **Haas BJ**, **Clemente JC**, **Quince C**, **Knight R**. UCHIME improves sensitivity and speed of chimera detection. *Bioinformatics* 27: 2194–2200, 2011.

16. **Edgar RC**. UPARSE: highly accurate OTU sequences from microbial amplicon reads. *Nat Methods* 10: 996–998, 2013.

17. **Fu ZD**, **Csanaky IL**, **Klaassen CD**. Gender-divergent profile of bile acid homeostasis during aging of mice. *PLoS ONE* 7: e32551, 2012.

18. **Gälman C**, **Angelin B**, **Rudling M**. Bile acid synthesis in humans has a rapid diurnal variation that is asynchronous with cholesterol synthesis. *Gastroenterology* 129: 1445–1453, 2005.

19. **Gälman C**, **Angelin B**, **Rudling M**. Pronounced variation in bile acid synthesis in humans is related to gender, hypertriglyceridaemia and circulating levels of fibroblast growth factor 19. *J Intern Med* 270: 580–588, 2011.

20. **Glaeser H**, **Bailey DG**, **Dresser GK**, **Gregor JC**, **Schwarz UI**, **McGrath JS**, **Jolicoeur E**, **Lee W**, **Leake BF**, **Tirona RG**, **Kim RB**. Intestinal drug transporter expression and the impact of grapefruit juice in humans. *Clin Pharmacol Ther* 81: 362–370, 2007.

21. **Hagenbuch B**, **Stieger B**. The SLCO (former SLC21) superfamily of transporters. *Molecular Aspects of Medicine* 34: 396–412, 2013.

22. **Hansen M**, **Scheltema MJ**, **Sonne DP**, **Hansen JS**, **Sperling M**, **Rehfeld JF**, **Holst JJ**, **Vilsbøll T**, **Knop FK**. Effect of chenodeoxycholic acid and the bile acid sequestrant colesevelam on glucagon-like peptide-1 secretion. *Diabetes Obes Metab* 18: 571–580, 2016.

23. **Ho JE**, **Larson MG**, **Vasan RS**, **Ghorbani A**, **Cheng S**, **Rhee EP**, **Florez JC**, **Clish CB**, **Gerszten RE**, **Wang TJ**. Metabolite profiles during oral glucose challenge. *Diabetes* 62: 2689–2698, 2013.

562 24. **Houten SM**, **Watanabe M**, **Auwerx J**. Endocrine functions of bile acids. *EMBO J* 25:
563 1419–1425, 2006.

564 25. **Huang A**, **Martin ER**, **Vance JM**, **Cai X**. Detecting genetic interactions in pathway-
565 based genome-wide association studies. *Genet Epidemiol* 38: 300–309, 2014.

566 26. **Jost L**. Partitioning diversity into independent alpha and beta components. *Ecology*
567 88: 2427–2439, 2007.

568 27. **Katsuma S**, **Hirasawa A**, **Tsujimoto G**. Bile acids promote glucagon-like peptide-1
569 secretion through TGR5 in a murine enteroendocrine cell line STC-1. *Biochem*
570 *Biophys Res Commun* 329: 386–390, 2005.

571 28. **Kawamata Y**, **Fujii R**, **Hosoya M**, **Harada M**, **Yoshida H**, **Miwa M**, **Fukusumi S**,
572 **Habata Y**, **Itoh T**, **Shintani Y**, **Hinuma S**, **Fujisawa Y**, **Fujino M**. A G protein-
573 coupled receptor responsive to bile acids. *J Biol Chem* 278: 9435–9440, 2003.

574 29. **Kelder T**, **Stroeve JHM**, **Bijlsma S**, **Radonjic M**, **Roeselers G**. Correlation network
575 analysis reveals relationships between diet-induced changes in human gut microbiota
576 and metabolic health. *Nutr Diabetes* 4: e122, 2014.

577 30. **Kreymann B**, **Williams G**, **Ghatei MA**, **Bloom SR**. Glucagon-like peptide-1 7-36: a
578 physiological incretin in man. *Lancet* 2: 1300–1304, 1987.

579 31. **Kumar P**, **Henikoff S**, **Ng PC**. Predicting the effects of coding non-synonymous
580 variants on protein function using the SIFT algorithm. *Nat Protoc* 4: 1073–1081, 2009.

581 32. **Lagkouvardos I**, **Fischer S**, **Kumar N**, **Clavel T**. Rhea: a transparent and modular R
582 pipeline for microbial profiling based on 16S rRNA gene amplicons. *PeerJ* 5: e2836,
583 2017.

584 33. **Lagkouvardos I**, **Kläring K**, **Heinzmann SS**, **Platz S**, **Scholz B**, **Engel K-H**,
585 **Schmitt-Kopplin P**, **Haller D**, **Rohn S**, **Skurk T**, **Clavel T**. Gut metabolites and
586 bacterial community networks during a pilot intervention study with flaxseeds in
587 healthy adult men. *Mol Nutr Food Res* 59: 1614–1628, 2015.

588 34. **Lee W**, **Glaeser H**, **Smith LH**, **Roberts RL**, **Moeckel GW**, **Gervasini G**, **Leake BF**,
589 **Kim RB**. Polymorphisms in human organic anion-transporting polypeptide 1A2
590 (OATP1A2): implications for altered drug disposition and central nervous system drug
591 entry. *J Biol Chem* 280: 9610–9617, 2005.

592 35. **Lefebvre P**, **Cariou B**, **Lien F**, **Kuipers F**, **Staels B**. Role of bile acids and bile acid
593 receptors in metabolic regulation. *Physiol Rev* 89: 147–191, 2009.

594 36. **Li H**, **Durbin R**. Fast and accurate long-read alignment with Burrows-Wheeler
595 transform. *Bioinformatics* 26: 589–595, 2010.

596 37. **Liddle RA**, **Goldfine ID**, **Rosen MS**, **Taplitz RA**, **Williams JA**. Cholecystokinin
597 bioactivity in human plasma. Molecular forms, responses to feeding, and relationship
598 to gallbladder contraction. *J Clin Invest* 75: 1144–1152, 1985.

599 38. **Ma K**, **Saha PK**, **Chan L**, **Moore DD**. Farnesoid X receptor is essential for normal

glucose homeostasis. *J Clin Invest* 116: 1102–1109, 2006.

39. **Maruyama T**, **Miyamoto Y**, **Nakamura T**, **Tamai Y**, **Okada H**, **Sugiyama E**, **Nakamura T**, **Itadani H**, **Tanaka K**. Identification of membrane-type receptor for bile acids (M-BAR). *Biochem Biophys Res Commun* 298: 714–719, 2002.

40. **Matysik S**, **Martin J**, **Bala M**, **Scherer M**, **Schäffler A**, **Schmitz G**. Bile acid signaling after an oral glucose tolerance test. *Chem Phys Lipids* 164: 525–529, 2011.

41. **McKenna A**, **Hanna M**, **Banks E**, **Sivachenko A**, **Cibulskis K**, **Kernytsky A**, **Garimella K**, **Altshuler D**, **Gabriel S**, **Daly M**, **DePristo MA**. The Genome Analysis Toolkit: a MapReduce framework for analyzing next-generation DNA sequencing data. *Genome Res* 20: 1297–1303, 2010.

42. **Nies AT**, **Niemi M**, **Burk O**, **Winter S**, **Zanger UM**, **Stieger B**, **Schwab M**, **Schaeffeler E**. Genetics is a major determinant of expression of the human hepatic uptake transporter OATP1B1, but not of OATP1B3 and OATP2B1. *Genome Med* 5: 1, 2013.

43. **Parks DJ**, **Blanchard SG**, **Bledsoe RK**, **Chandra G**, **Consler TG**, **Kliewer SA**, **Stimmel JB**, **Willson TM**, **Zavacki AM**, **Moore DD**, **Lehmann JM**. Bile acids: natural ligands for an orphan nuclear receptor. *Science* 284: 1365–1368, 1999.

44. **Popescu IR**, **Helleboid-Chapman A**, **Lucas A**, **Vandewalle B**, **Dumont J**, **Bouchaert E**, **Derudas B**, **Kerr-Conte J**, **Caron S**, **Pattou F**, **Staels B**. The nuclear receptor FXR is expressed in pancreatic beta-cells and protects human islets from lipotoxicity. *FEBS Lett* 584: 2845–2851, 2010.

45. **Renga B**, **Mencarelli A**, **Vavassori P**, **Brancaleone V**, **Fiorucci S**. The bile acid sensor FXR regulates insulin transcription and secretion. *Biochim Biophys Acta* 1802: 363–372, 2010.

46. **Ridlon JM**, **Kang D-J**, **Hylemon PB**. Bile salt biotransformations by human intestinal bacteria. *J Lipid Res* 47: 241–259, 2006.

47. **Rossi SS**, **Converse JL**, **Hofmann AF**. High pressure liquid chromatographic analysis of conjugated bile acids in human bile: simultaneous resolution of sulfated and unsulfated lithocholyl amidates and the common conjugated bile acids. *J Lipid Res*.

48. **Schmid A**, **Neumann H**, **Karrasch T**, **Liebisch G**, **Schäffler A**. Bile Acid Metabolome after an Oral Lipid Tolerance Test by Liquid Chromatography-Tandem Mass Spectrometry (LC-MS/MS). *PLoS ONE* 11: e0148869, 2016.

49. **Shaham O**, **Wei R**, **Wang TJ**, **Ricciardi C**, **Lewis GD**, **Vasan RS**, **Carr SA**, **Thadhani R**, **Gerszten RE**, **Mootha VK**. Metabolic profiling of the human response to a glucose challenge reveals distinct axes of insulin sensitivity. *Mol Syst Biol* 4: 214, 2008.

50. **Sonne DP**, **Rehfeld JF**, **Holst JJ**, **Vilsbøll T**, **Knop FK**. Postprandial gallbladder emptying in patients with type 2 diabetes: potential implications for bile-induced secretion of glucagon-like peptide 1. *Eur J Endocrinol* 171: 407–419, 2014.

640 51. **Sonne DP**, **Samuel van Nierop F**, **Kulik W**, **Soeters MR**, **Vilsbøll T**, **Knop FK**.
641 Postprandial Plasma Concentrations of Individual Bile Acids and FGF-19 in Patients
642 with Type 2 Diabetes. *J Clin Endocrinol Metab* (June 7, 2016). doi: 10.1210/jc.2016-
643 1607.

644 52. **Steiner C**, **Othman A**, **Saely CH**, **Rein P**, **Drexel H**, **Eckardstein von A**, **Rentsch**
645 **KM**. Bile acid metabolites in serum: intraindividual variation and associations with
646 coronary heart disease, metabolic syndrome and diabetes mellitus. *PLoS ONE* 6:
647 e25006, 2011.

648 53. **Tagliacozzi D**, **Mozzi AF**, **Casetta B**, **Bertucci P**, **Bernardini S**, **Di Ilio C**, **Urbani A**,
649 **Federici G**. Quantitative analysis of bile acids in human plasma by liquid
650 chromatography-electrospray tandem mass spectrometry: a simple and rapid one-
651 step method. *Clin Chem Lab Med* 41: 1633–1641, 2003.

652 54. **Trauner M**, **Boyer JL**. Bile Salt Transporters: Molecular Characterization, Function,
653 and Regulation. *Physiol Rev* 83: 633–671, 2003.

654 55. **Turley SD**, **Schwarz M**, **Spady DK**, **Dietschy JM**. Gender-related differences in bile
655 acid and sterol metabolism in outbred CD-1 mice fed low- and high-cholesterol diets -
656 Turley - 2003 - Hepatology - Wiley Online Library. *Hepatology*.

657 56. **Vanitha Bala SRDPKADNSMAJSJRGKSM**. Release of GLP-1 and PYY in response
658 to the activation of G protein-coupled bile acid receptor TGR5 is mediated by
659 Epac/PLC-ε pathway and modulated by endogenous H2S. *Frontiers in Physiology* 5,
660 2014.

661 57. **Wang H**, **Chen J**, **Hollister K**, **Sowers LC**, **Forman BM**. Endogenous bile acids are
662 ligands for the nuclear receptor FXR/BAR. *Mol Cell* 3: 543–553, 1999.

663 58. **Wang K**, **Li M**, **Hakonarson H**. ANNOVAR: functional annotation of genetic variants
664 from high-throughput sequencing data. *Nucleic Acids Res* 38: e164, 2010.

665 59. **Wang Q**, **Garrity GM**, **Tiedje JM**, **Cole JR**. Naive Bayesian classifier for rapid
666 assignment of rRNA sequences into the new bacterial taxonomy. *Appl Environ*
667 *Microbiol* 73: 5261–5267, 2007.

668 60. **Watanabe M**, **Houten SM**, **Mataki C**, **Christoffolete MA**, **Kim BW**, **Sato H**,
669 **Messaddeq N**, **Harney JW**, **Ezaki O**, **Kodama T**, **Schoonjans K**, **Bianco AC**,
670 **Auwerx J**. Bile acids induce energy expenditure by promoting intracellular thyroid
671 hormone activation. *Nature* 439: 484–489, 2006.

672 61. **Watanabe M**, **Houten SM**, **Wang L**, **Moschetta A**, **Mangelsdorf DJ**, **Heyman RA**,
673 **Moore DD**, **Auwerx J**. Bile acids lower triglyceride levels via a pathway involving
674 FXR, SHP, and SREBP-1c. *J Clin Invest* 113: 1408–1418, 2004.

675 62. **Wegner K**, **Just S**, **Gau L**, **Mueller H**, **Gérard P**, **Lepage P**, **Clavel T**, **Rohn S**.
676 Rapid analysis of bile acids in different biological matrices using LC-ESI-MS/MS for
677 the investigation of bile acid transformation by mammalian gut bacteria. *Anal Bioanal*
678 *Chem* 409: 1231–1245, 2017.

679 63. **Xiang X**, **Backman JT**, **Neuvonen PJ**, **Niemi M**. Gender, but not CYP7A1 or

SLCO1B1 polymorphism, affects the fasting plasma concentrations of bile acids in human beings. *Basic Clin Pharmacol Toxicol* 110: 245–252, 2012.

64. **Yamagata K**, **Daitoku H**, **Shimamoto Y**, **Matsuzaki H**, **Hirota K**, **Ishida J**, **Fukamizu A**. Bile acids regulate gluconeogenic gene expression via small heterodimer partner-mediated repression of hepatocyte nuclear factor 4 and Foxo1. *J Biol Chem* 279: 23158–23165, 2004.

65. **Zhao X**, **Peter A**, **Fritsche J**, **Elcnerova M**, **Fritsche A**, **Häring H-U**, **Schleicher ED**, **Xu G**, **Lehmann R**. Changes of the plasma metabolome during an oral glucose tolerance test: is there more than glucose to look at? *Am J Physiol Endocrinol Metab* 296: E384–93, 2009.

66. **Zietak M**, **Kozak LP**. Bile acids induce uncoupling protein 1-dependent thermogenesis and stimulate energy expenditure at thermoneutrality in mice. *Am J Physiol Endocrinol Metab* (December 29, 2015). doi: 10.1152/ajpendo.00485.2015.

Figure Legends

Table 1 – List of selected genes known as involved in BA synthesis and transport that were screened for deleterious variations. Genes selected represent hormones, membrane receptors, transcription factors and enzymes involved in BA synthesis as well as transporters expressed in hepatocytes, bile canaliculi and intestine.

Table 2 – Effect of different parameters identified by multivariate analyses as responsible for the observed variation in the most abundant bile acids in plasma in postprandial state. The numbers in each cell indicate the proportion of variation (in percentage) in each BA explained by the corresponding variable. The numbers in brackets after gene names indicate the number of subjects carrying variations in the respective gene. Highlighted cells indicate significant associations ($P<0.05$).

Figure 1 – The energy restriction did not affect BA profiles during OGTT and MMTT or after a 12-hour fasting. A – Total BA in plasma during the OGTT. B – Total BA in plasma during the MMTT. Continuous lines represent BA profile before and dotted lines, the BA profile after a 12 weeks period of intervention with 20% dietary energy restriction. Only the volunteers that abide to the energy restriction are represented (in control group no changes due to the energy restriction were observed as well). C – Total BA and BA classes in plasma after a 12-hour fasting. N = 40.

Figure 2 – Fasting plasma bile acids. Plasma concentrations of the most abundant BA in healthy subjects in the overnight fasting state (average of sampling performed at t=0 of OGTT and MMTT before and after the weight loss intervention). Each differently colored segment in bars represents the concentration of an individual BA.

Figure 3 – Plasma BA concentration profiles in response to the OGTT and MMTT. A to **F** - Plasma concentrations of different BA classes during the OGTT (dotted line) and MMTT (full line). **G** and **H** – Changes in the composition of the plasma BA pool according to their conjugation type during the OGTT (G) and MMTT (H). Results are shown as the mean ± SEM of all volunteers averaging the results of the two challenges performed before and after 12 weeks (n=72).

Figure 4 – Gender effects on plasma BA concentration profiles during the OGTT and MMTT.

A to **C** – Plasma concentrations of total, glycine- and taurine-conjugated BA in men (dotted lines, n=35) and women (full lines, n=37) during the OGTT. **D** to **F** – Plasma concentrations of total, glycine- and taurine-conjugated BA in men (dotted lines, n=35) and women (full lines, n=37) during the MMTT. Results are shown as the mean ± SEM, averaging the results of challenges performed before and after intervention. Significant differences in the AUC after t- test are indicated in the graphs.

Figure 5 – Clustering of volunteers according to postprandial plasma BA kinetics.

A – Clustering of volunteers based on plasma concentration profiles of bile acids during the MMTT. **B** – Changes in total and different classes of bile acids during the MMTT in participants of the 3 clusters. Results are expressed as mean ± SEM. n=35 in cluster 1, n=13 in cluster 2 and n=21 in cluster 3. **C** – Summary of differences found among the 3 clusters for the different bile acid classes as represented in pane B (P≤0.05).

Figure 6 – Effects of the functional polymorphism A516C in *SLCO1A2* (OATP1A2) on plasma BA kinetics. A to C – Plasma concentrations of bile acids in A516C carriers (dotted line, n=9) and non-carriers (full line, n=62) during the MMTT. **D to F** – Plasma concentrations of bile acids in A516C carriers and non-carriers during the OGTT. Results are the mean ± SEM of BA levels averaging the results of challenges performed before and after the weight loss intervention. Statistical differences (multiple T-tests) are indicated in each graph. The grey area in panes C and F represents the profile of glucose during the MMTT and OGTT, respectively.

Figure 7 – *De novo* clustering analysis of fecal microbiota profiles as obtained by high-throughput sequencing of 16S rRNA gene amplicons. Partitioning Around Medoids was performed as described previously. The clustering with best support was visualized with an NMDS plot (**A**). Associated changes in alpha-diversity (**B**) and differential abundances of taxonomic groups among the clusters (**C**) were tested statistically in the R programming environment using Rhea.

Figure 8 – Relationship between plasma bile acids and GLP-1 concentrations in the post-prandial state. A and B – Plasma concentrations of glycine-conjugated BA (black

lines) and GLP-1 (grey lines) in response to the OGTT (A) and MMTT (B) (N=72). **C and D** – Plasma concentration of glycine-conjugated BA (black lines) and GLP-1 (grey lines). Subjects were ranked according to post-prandial increase of glycine-conjugated BA concentrations during the first hour of the OGTT (C) and MMTT (D) (N=36 in each group). Results are expressed as mean ± SEM of BA fold-change from t=0.

Protein Name	Symbol	Gene symbol	Function
Cholesterol 7α-hydroxylase	CYP7A1	CYP7A1	Enzyme
Sterol 27-hydroxylase	CYP27A1	CYP27A1	Enzyme
25-hydroxycholesterol 7α-hydroxylase	CYP7B1	CYP7B1	Enzyme
24-hydroxycholesterol 7α-hydroxylase	CYP39A1	CYP39A1	Enzyme
Microsomal 3β-hydroxy-Δ5-C27-steroid oxidoreductase	HSD3B7	HSD3B7	Enzyme
Microsomal sterol 12α-hydroxylase	CYP8B1	CYP8B1	Enzyme
Δ4-3-oxosteroid 5β-reductase	AKR1D1	AKR1D1	Enzyme
Acyl-CoA Oxidase 1	ACOX1	ACOX1	Enzyme
Acyl-CoA Oxidase 2	ACOX2	ACOX2	Enzyme
Bile Acid-CoA:Amino Acid N-Acyltransferase	BAAT	BAAT	Enzyme
Bile Acid-CoA Ligase	BAL	SLC27A5	Enzyme
α-Methylacyl-CoA Racemase	AMACR	AMACR	Enzyme
D-bifunctional enzyme	DBP	DBP	Enzyme
Peroxisomal Thiolase 2	SCP2	SCP2	Enzyme
Aldo-Keto Reductase Family 1 Member C4	AKR1C4	AKR1C4	Enzyme
Hydroxysteroid Sulfotransferase	HST	SULT2A1	Enzyme
UDP glucuronosyltransferase Family 2 Member B4	UGT2B4	UGT2B4	Enzyme
UDP glucuronosyltransferase Family 2 Member B7	UGT2B7	UGT2B7	Enzyme
UDP glucuronosyltransferase Family 1 Member A3	UGT1A3	UGT1A3	Enzyme
Solute Carrier Family 4 Member 2	SLC4A2	SLC4A2	Enzyme
Microsomal Epoxide Hydrolase	mEH	EPHX1	Enzyme
Cholecystokinin	CCK	CCK	Hormone
Fobroblast Growth Factor 19	FGF19	FGF19	Hormone
Farnesoid X Receptor	FXR	NR1H4	Nuclear receptor
Small Heterodimer Partner	SHP	NR0B2	Nuclear receptor
Liver X Receptor	LXR	NR1H3	Nuclear receptor
Forkhead Box A2	HNF-3β	FOXA2	Nuclear receptor
Hepatocyte Nuclear Factor-4α	HNF-4α	HNF4A	Nuclear receptor
G Protein-Coupled Bile Acid Receptor 1	GPBAR1	GPBAR1	Receptor
Bile Salt Export Pump	BSEP	ABCB11	Transporter
Apical Sodium-dependent BA Transporter	ASBT	SLC10A2	Transporter
Organic Solute Transporter-α subunit	OSTα	SLC51A	Transporter
Organic Solute Transporter-β subunit	OSTβ	SLC51B	Transporter
Sodium/Taurocholate Cotransporting Polypeptide	NTCP	SLC10A1	Transporter
Solute Carrier Organic Anion transporter Family Member 1A2	OATP1A2	SLCO1A2	Transporter
Solute Carrier Organic Anion transporter Family Member 1B1	OATP1B1	SLCO1B1	Transporter
Solute Carrier Organic Anion transporter Family Member 1B3	OATP1B3	SLCO1B3	Transporter
Solute Carrier Organic Anion transporter Family Member 2B1	OATP2B1	SLCO2B1	Transporter
ATP Binding Cassette Subfamily C Member 3	ABCC3	ABCC3	Transporter
ATP Binding Cassette Subfamily A Member 1	ABCA1	ABCA1	Transporter
ATP Binding Cassette Subfamily A Member 3	ABCA3	ABCA3	Transporter
ATP Binding Cassette Subfamily G Member 2	ABCG2	ABCG2	Transporter
ATP Binding Cassette Subfamily G Member 5	ABCG5	ABCG5	Transporter
ATP Binding Cassette Subfamily G Member 8	ABCG8	ABCG8	Transporter
ATP Binding Cassette Subfamily C Member 2	ABCC2	ABCC2	Transporter
ATP Binding Cassette Subfamily B Member 1	ABCB1	ABCB1	Transporter
ATP Binding Cassette Subfamily B Member 4	ABCB4	ABCB4	Transporter
ATPase Phospholipid Transporting 8B1	ATP8B1	ATP8B1	Transporter
Cytosolic Intestinal BA-binding Protein	IBABP	FABP6	Transporter

	TIME	GENDER	genetic explained variation	microbiome explained variation	CYP27A1 (4)	CYP39A1 (24)	HSD3B7 (4)	SLC10A2 (4)	SLCO1A2 (9)	SLCO1B1 (30)	SLCO1B3 (24)	ABCC3 (63)	ABCA3 (4)	ABCG5 (10)	ABCG8 (6)	ABCC2 (8)	AMACR (63)	GPBAR1 (6)	EPHX1 (39)	UGT2B4 (49)	ATP8B1 (26)	NR0B2 (10)	Acidaminococcaceae	Alcaligenaceae	Bacteroidaceae	Bifidobacteriaceae	Christensenellaceae	Coriobacteriaceae	Erysipelotrichaceae	Lachnospiraceae	Peptostreptococcaceae	Porphyromonadaceae	Prevotellaceae	Rikenellaceae	Ruminococcaceae	Veillonellaceae	TOTAL VARIATION EXPLAINED
CA	**2**	**1**	**39**	**21**	0	3	1	5	1	1	3	9	0	0	2	0	2	6	2	1	3	0	0	0	0	0	0	0	5	1	12	2	0	0	0	1	**63**
CDCA	**6**	**1**	**38**	**10**	0	2	2	3	0	0	2	4	0	0	0	0	4	6	3	3	8	1	2	0	1	0	0	1	2	0	3	0	0	0	1	0	**55**
DCA	**4**	**0**	**54**	**11**	0	0	0	3	0	3	1	6	2	2	2	4	8	2	14	1	1	5	2	1	2	1	0	2	0	1	0	0	1	0	0	1	**69**
GCA	**14**	**0**	**23**	**6**	0	1	0	0	3	0	2	1	1	0	1	1	3	1	2	3	4	0	1	0	1	1	0	0	0	0	1	0	0	1	1	0	**43**
GCDCA	**21**	**1**	**18**	**8**	0	1	0	0	0	0	2	0	2	0	0	0	3	2	3	0	3	2	1	0	2	1	0	4	0	0	0	0	0	0	0	0	**48**
GDCA	**10**	**1**	**50**	**2**	0	0	1	0	1	3	2	2	3	0	3	1	2	0	29	1	1	1	0	0	0	0	0	0	0	0	0	0	0	0	1	1	**63**
TCA	**5**	**3**	**25**	**4**	0	0	3	1	2	1	3	1	0	0	0	1	6	1	0	2	4	0	0	0	0	1	1	0	0	0	0	0	0	0	2	0	**37**
TCDCA	**13**	**5**	**24**	**6**	0	0	2	3	1	0	2	2	0	1	0	0	4	2	2	1	2	2	1	0	0	0	1	4	0	0	0	0	0	0	0	0	**48**
TDCA	**7**	**4**	**50**	**3**	0	0	0	2	0	1	3	2	2	1	2	1	3	1	31	1	0	0	0	0	1	0	0	0	0	0	0	0	0	0	1	1	**64**

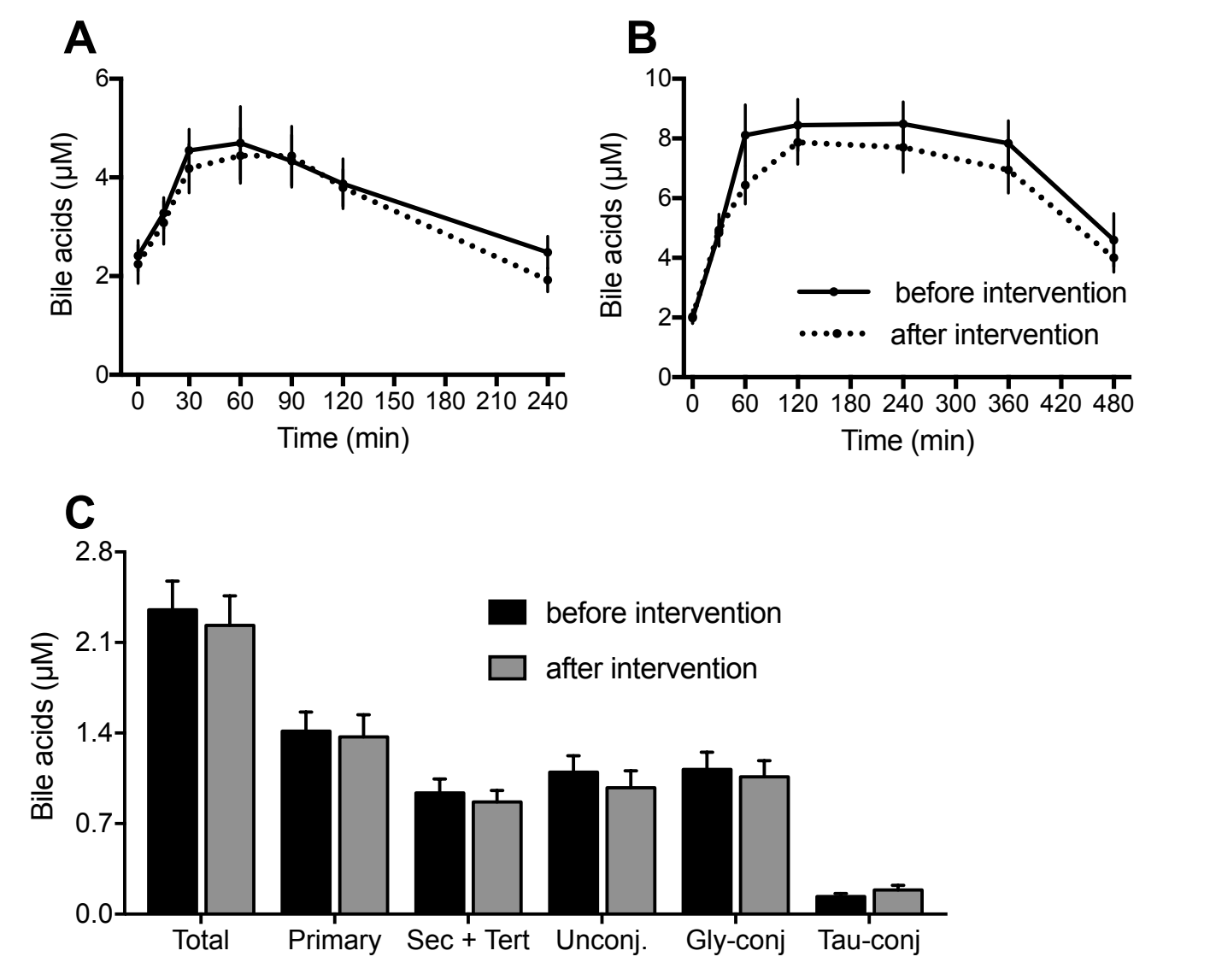
A
Bile acids (µM)
0
2
4
6
0 30 60 90 120 150 180 210 240
Time (min)
B
Bile acids (µM)
0
2
4
6
8
10
0 60 120 180 240 300 360 420 480
Time (min)
before intervention
after intervention
C
Bile acids (µM)
0.0
0.7
1.4
2.1
2.8
before intervention
after intervention
Total
Primary
Sec + Tert
Unconj.
Gly-conj
Tau-conj

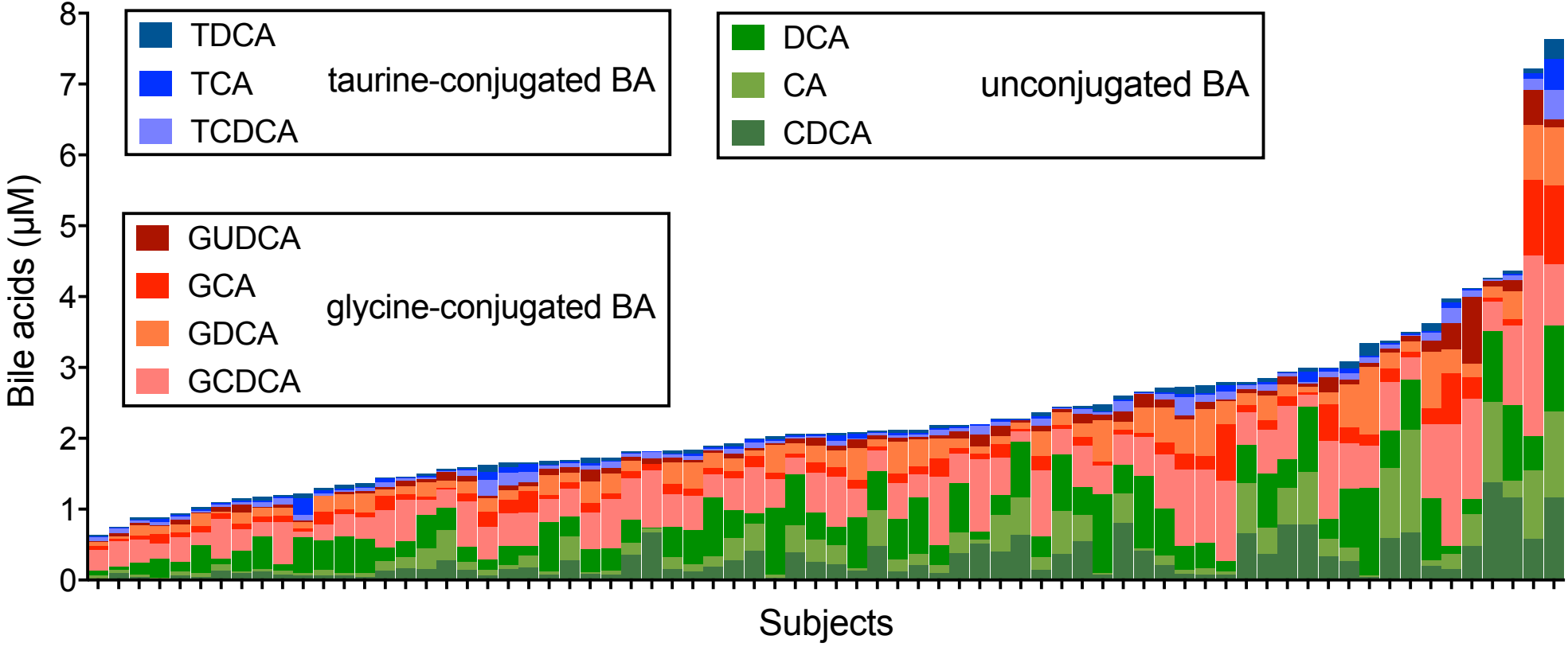
TDCA
TCA
TCDCA
taurine-conjugated BA
DCA
CA
CDCA
unconjugated BA
GUDCA
GCA
GDCA
GCDCA
glycine-conjugated BA
Bile acids (μM)
0
1
2
3
4
5
6
7
8
Subjects

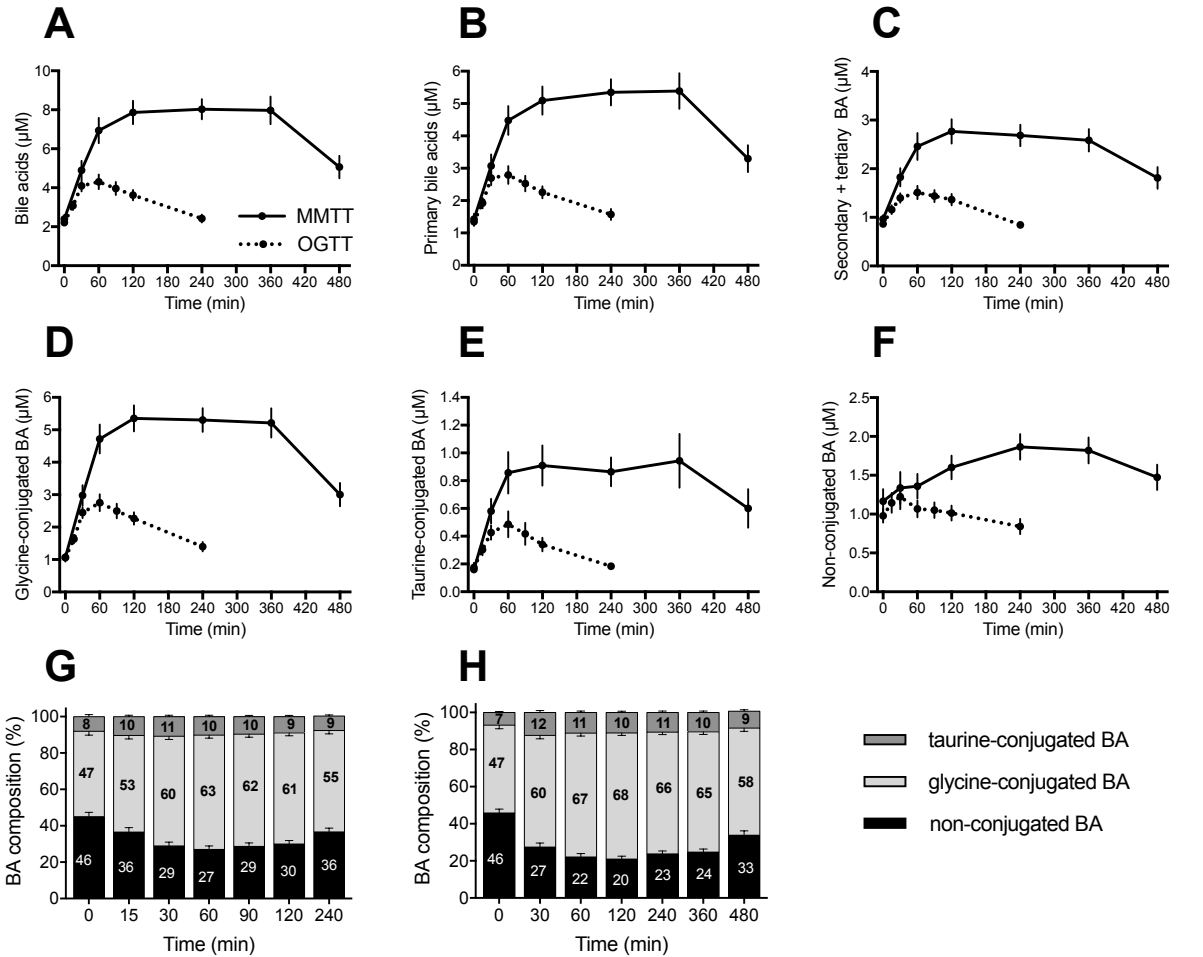
A
Bile acids (μM)
MMTT
OGTT
Time (min)
B
Primary bile acids (μM)
Time (min)
C
Secondary + tertiary BA (μM)
Time (min)
D
Glycine-conjugated BA (μM)
Time (min)
E
Taurine-conjugated BA (μM)
Time (min)
F
Non-conjugated BA (μM)
Time (min)
G
BA composition (%)
8 10 11 10 10 9 9
47 53 60 63 62 61 55
46 36 29 27 29 30 36
Time (min)
H
BA composition (%)
7 12 11 10 11 10 9
47 60 67 68 66 65 58
46 27 22 20 23 24 33
Time (min)
taurine-conjugated BA
glycine-conjugated BA
non-conjugated BA

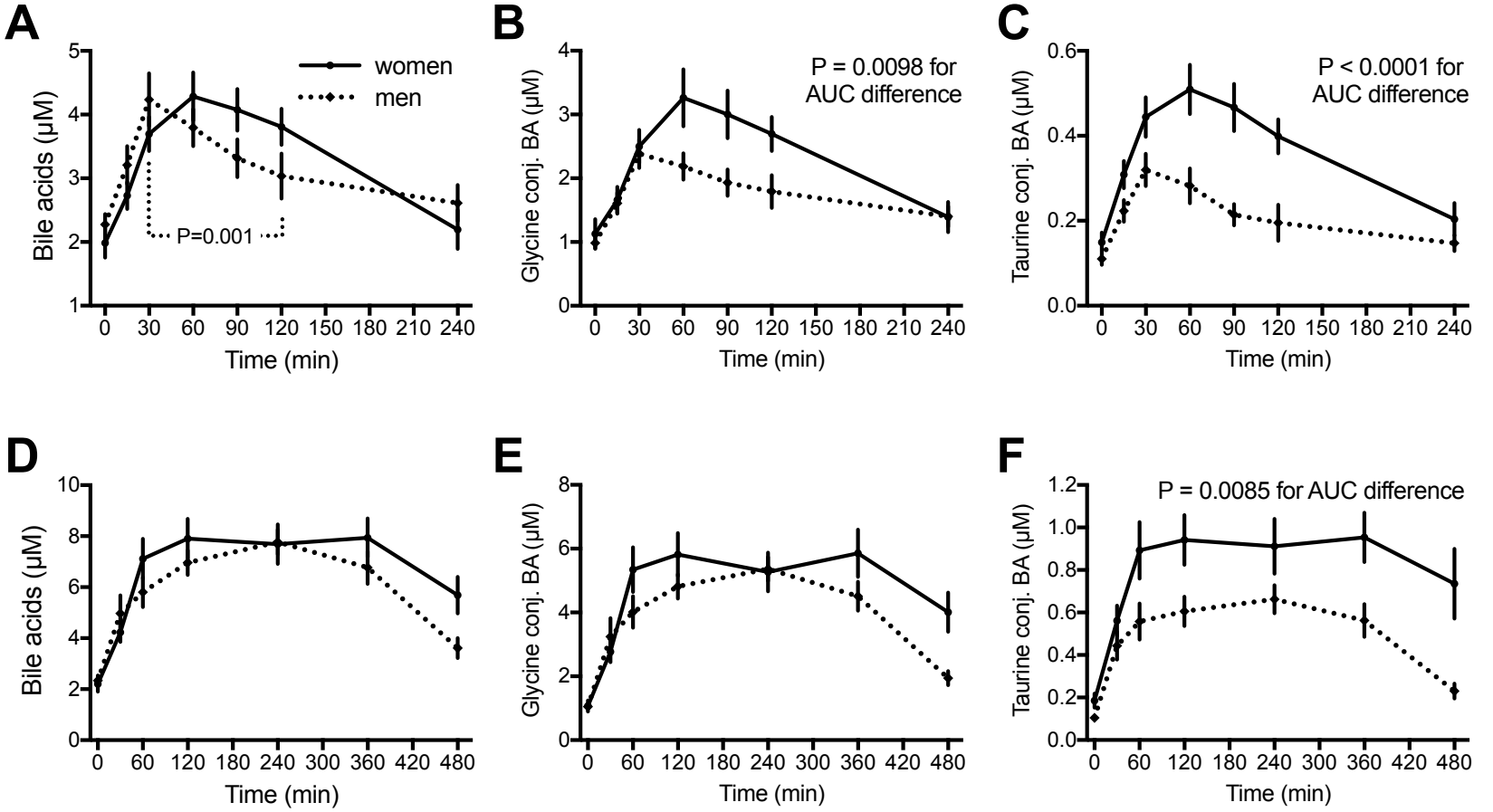
A
B
C
D
E
F
Bile acids (μM)
Glycine conj. BA (μM)
Taurine conj. BA (μM)
Time (min)
women
men
P=0.001
P = 0.0098 for AUC difference
P < 0.0001 for AUC difference
P = 0.0085 for AUC difference

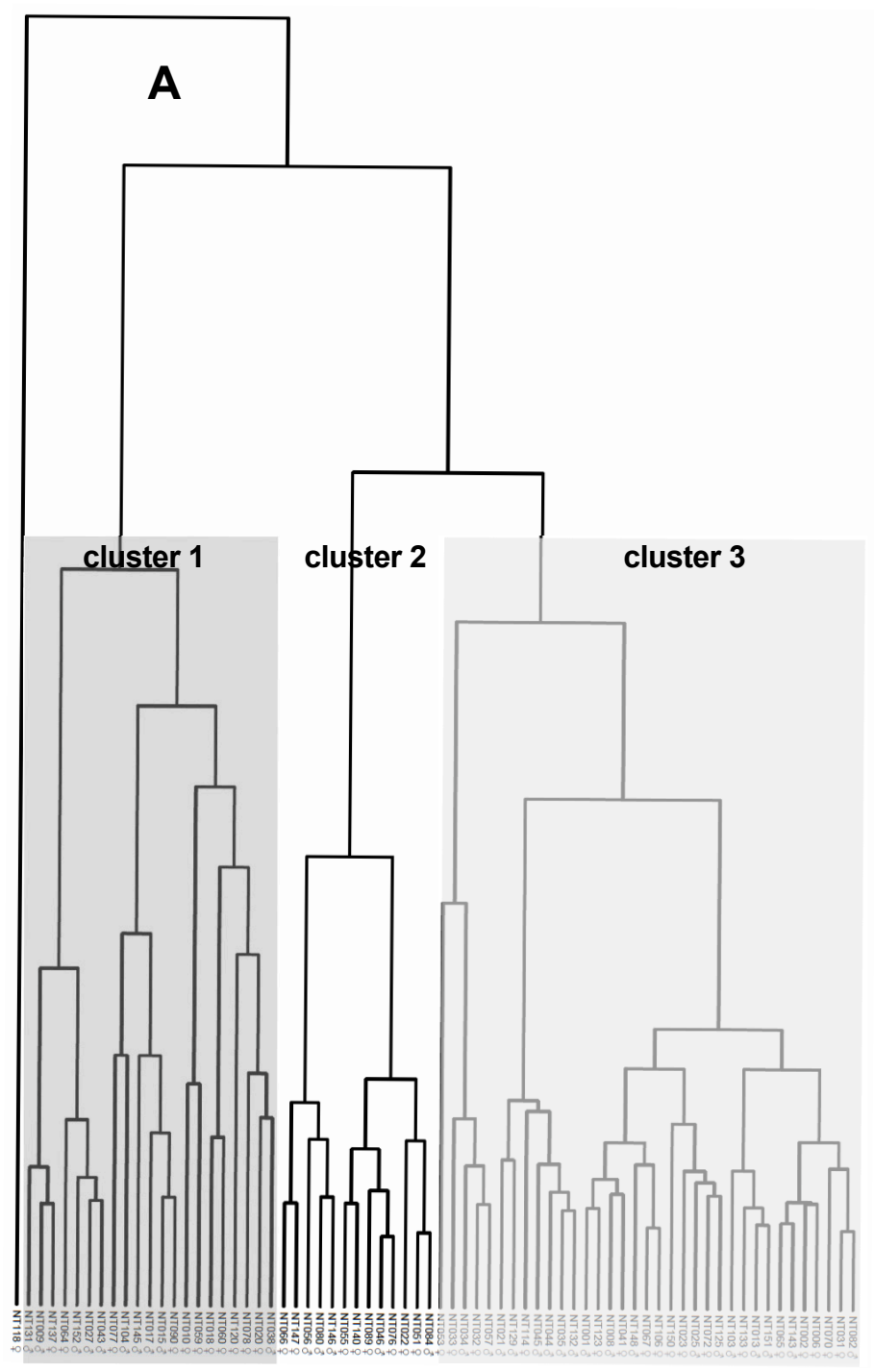

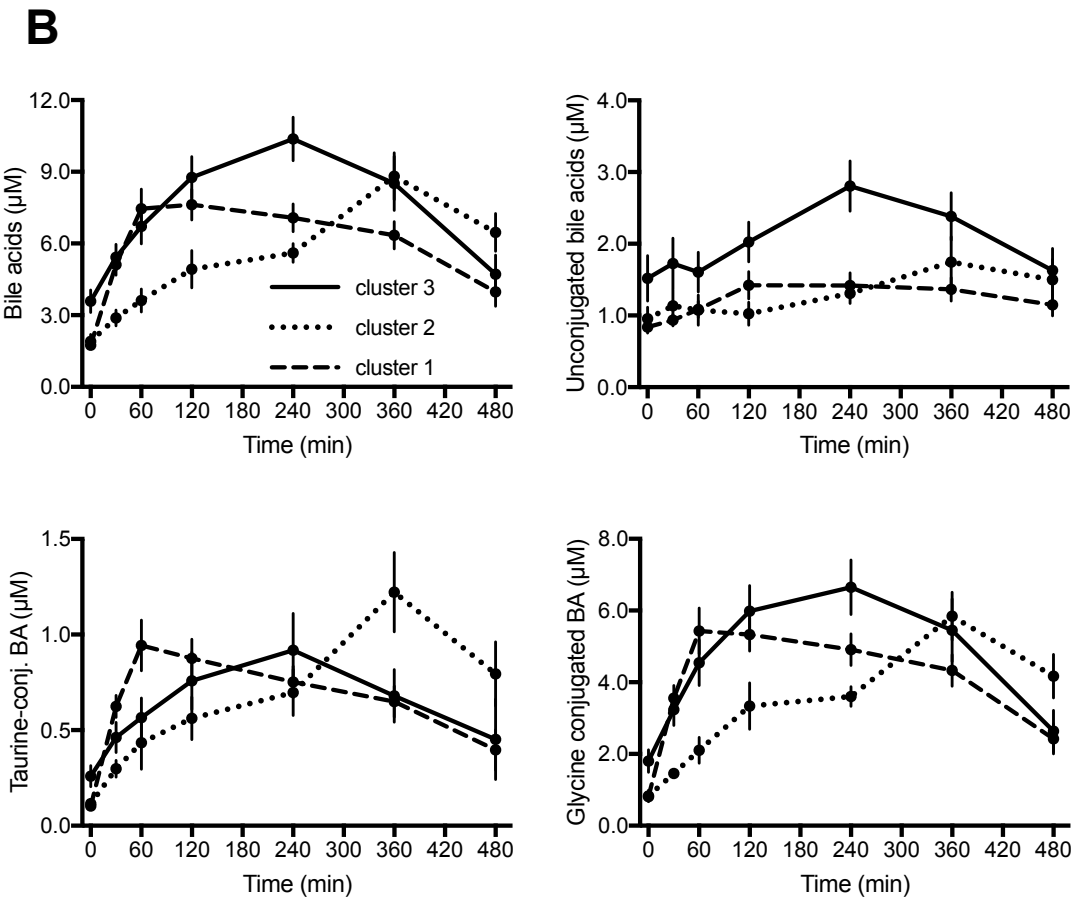

C

	total	unconj.	glycine-conj.	taurine-conj.
0	3≠1	3≠1	-	-
30	3≠2, 2≠1	3≠1	3≠2, 2≠1	-
60	3≠2, 2≠1	-	3≠2, 2≠1	3≠1, 2≠1
120	3≠2, 2≠1	3≠2, 3≠1	3≠2, 2≠1	-
240	3≠2, 3≠1	3≠2, 3≠1	3≠2, 3≠1	-
360	3≠1, 2≠1	3≠1	-	3≠2, 2≠1
480	2≠1	-	2≠1	2≠1

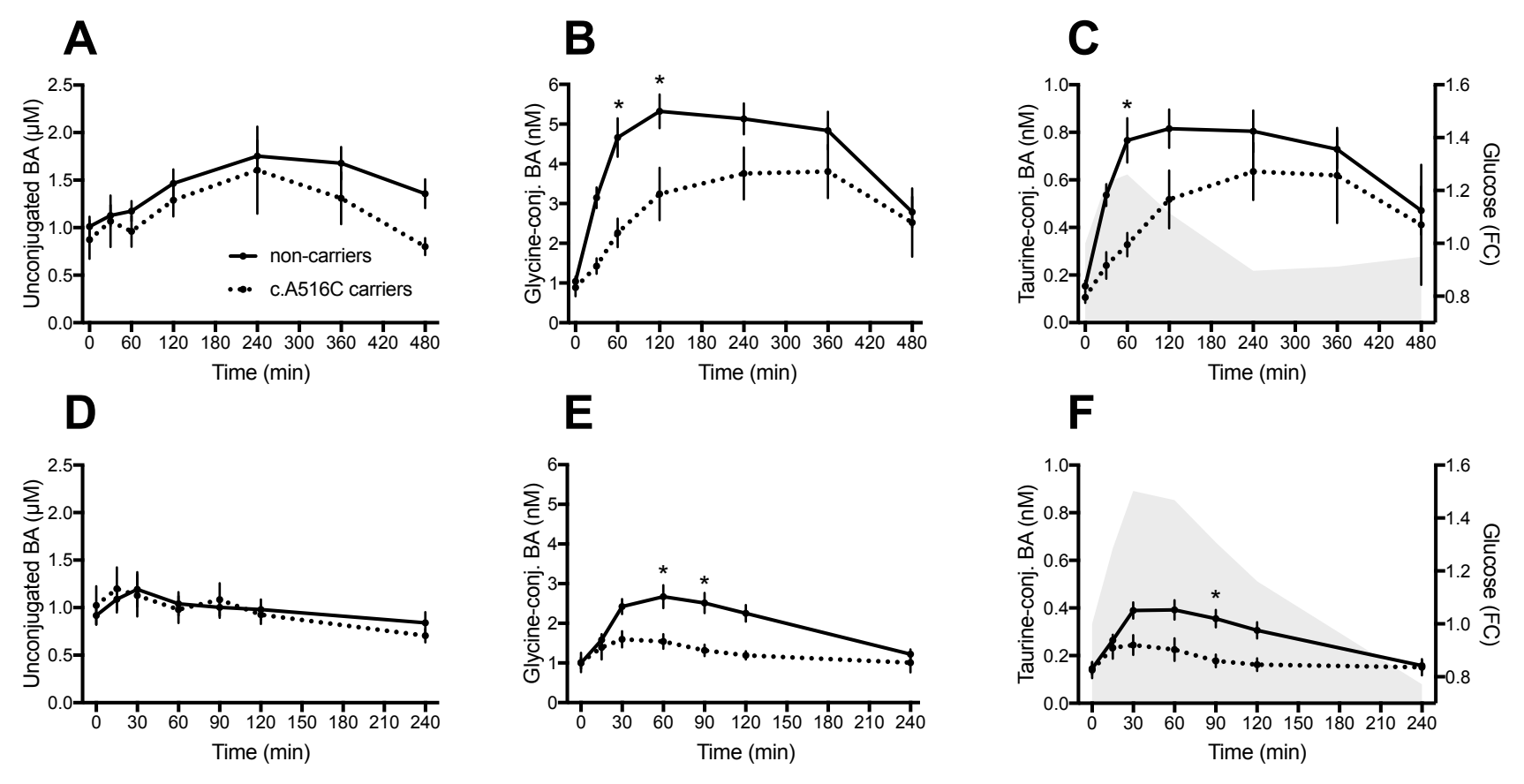
A
B
C
D
E
F
Unconjugated BA (μM)
Glycine-conj. BA (nM)
Taurine-conj. BA (nM)
Glucose (FC)
Time (min)
non-carriers
c.A516C carriers
*

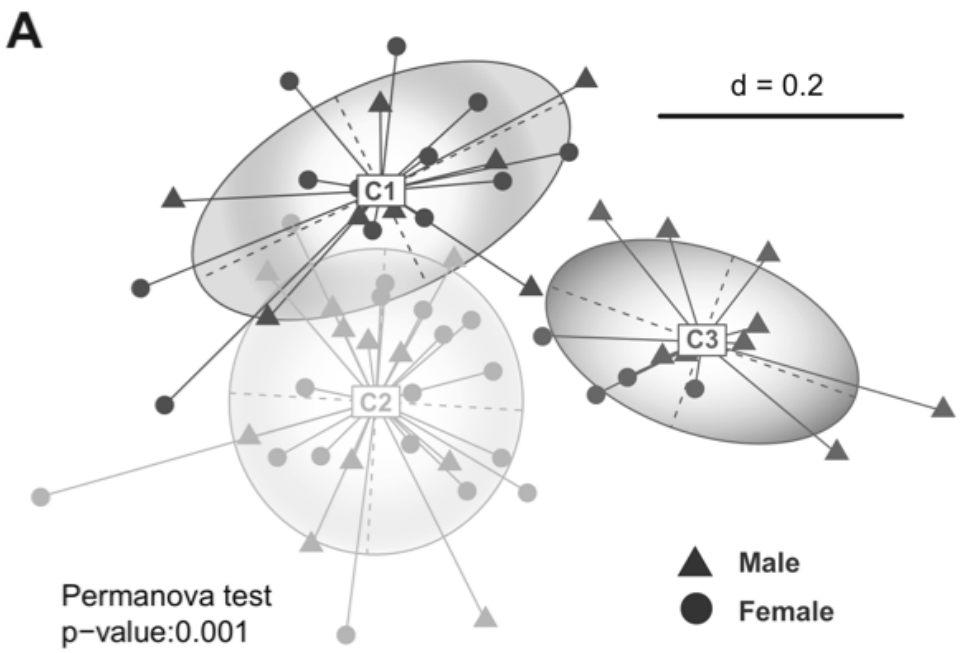

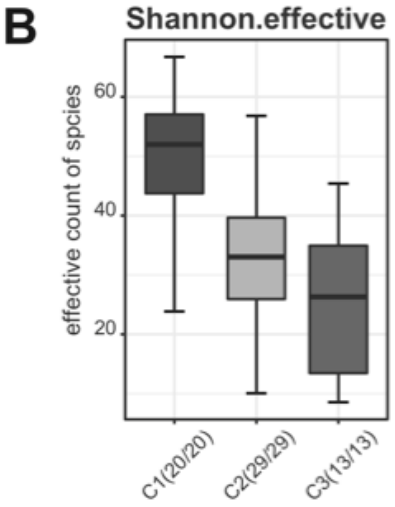

Wilcoxon Rank Sum Test − pairwise

Cluster	P−value	Adj. p−value
1−2	1e−04	2e−04
1−3	1e−04	2e−04

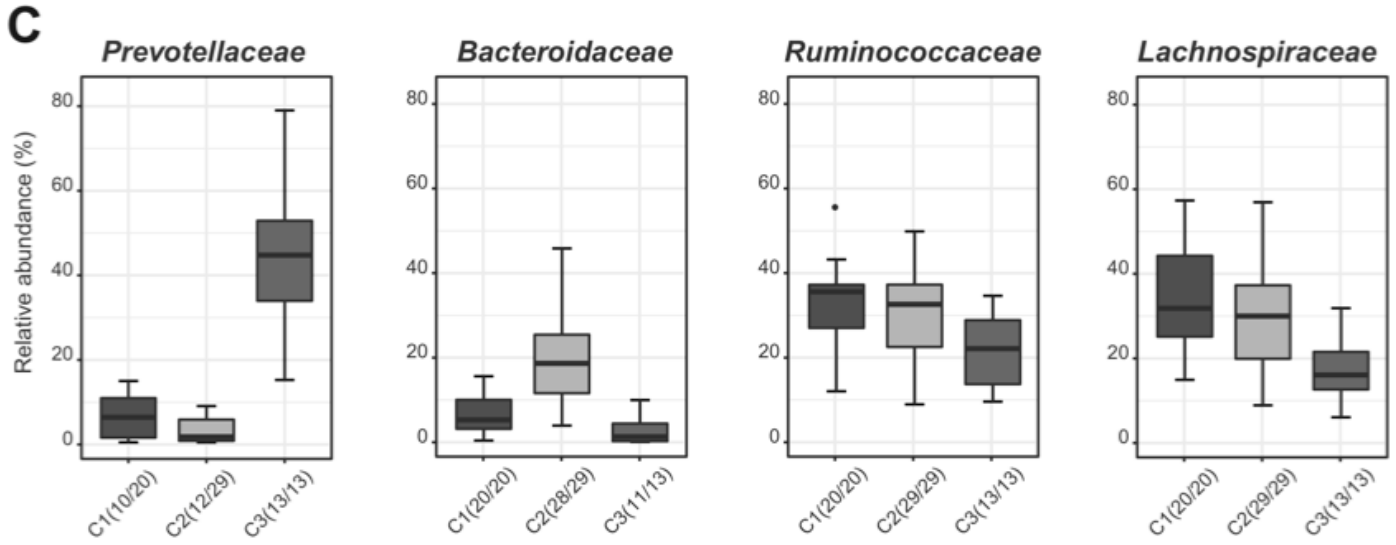

Wilcoxon Rank Sum Test − pairwise

Cluster	P−value	Adj. p−value
1−3	0	0
2−3	0	0

Wilcoxon Rank Sum Test − pairwise

Cluster	P−value	Adj. p−value
1−2	0.000	0.000
1−3	0.014	0.014
2−3	0.000	0.000

Wilcoxon Rank Sum Test − pairwise

Cluster	P−value	Adj. p−value
1−3	0.0008	0.0024
2−3	0.0130	0.0195

Wilcoxon Rank Sum Test − pairwise

Cluster	P−value	Adj. p−value
1−3	0.0002	0.0006
2−3	0.0028	0.0042

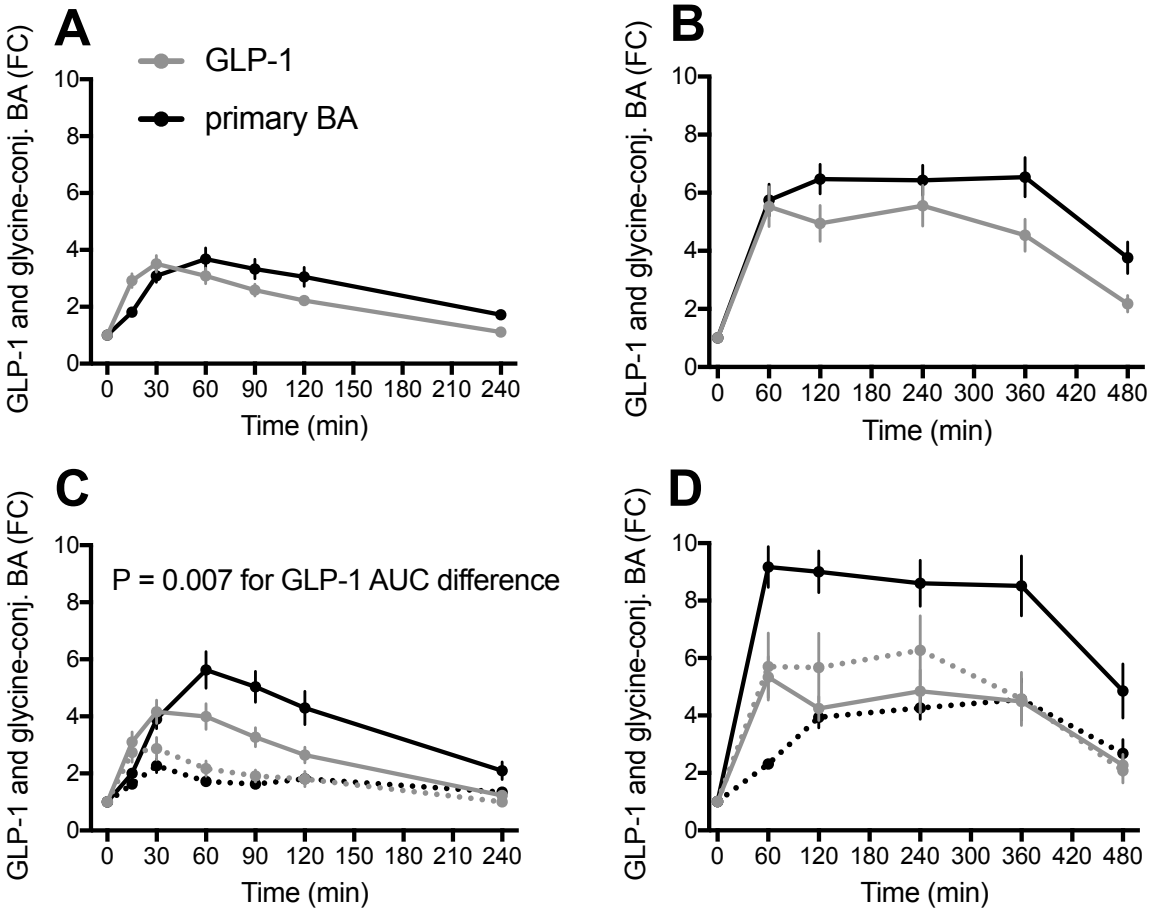
A
GLP-1
primary BA
GLP-1 and glycine-conj. BA (FC)
Time (min)
B
C
P = 0.007 for GLP-1 AUC difference
D
GLP-1 in subjects with **low** post-prandial BA increase
GLP-1 in subjects with **high** post-prandial BA increase
BA in subjects with **low** post-prandial BA increase
BA in subjects with **high** post-prandial BA increase